JOURNAL OF PETROLEUM AND MINING
مجلة النفط والتعدين

Developing Experimental Petrophysical Relationships for Geological Stratigraphic Succession (Hartha- Fatha Formations) in the East Baghdad Oil Field

Maan H. Abdullah Al-majid

Department of Mining Engineering, College of Petroleum and Mining Engineering, University of Mosul, Iraq

Article information

Article history:
Received: Apr 04, 2025
Revised: Jun 05, 2025
Accepted: Jun 24, 2025
Available Online: Jul 01, 2025

Keywords:
velocity analyses
porosity
density
empirical equations
oil field

Correspondence:
Name: **Maan H. Abdullah Al-majid**
maan.abdalla@uomosul.edu.iq

ABSTRACT

The present study deals with experimental mathematical equations that link density and porosity with depth. After obtaining the density and porosity information from five well logs scattered in the East Baghdad oil field, new empirical equations (porosity-depth, density-depth) were produced for all the geological formations within the period between the Fatha and Hartha Formations. The correlation coefficient (R) of these equations derived for each formation ranged from 0.06 to 0.87, which was attributed to variable lithology effects. The depth information of (126) velocity analyses situated at the seismic lines grid covering the field had been used for applying the new equations. After the new empirical equations were applied to the whole field, porosity and density contour maps for the period (Fatha- Hartha) were produced. The locations of high porosity zones were identified and related to the compaction and petroleum distribution in the field.

DOI: **********,

إستحداث علاقات بيتروفيزيائية تجريبية للتعاقب الجيولوجي الطباقي (بين تكويني الفتحة و الحارثة) في حقل شرق بغداد النفطي

معن حسن عبد الله

قسم هندسة التعدين، كلية هندسة النفط والتعدين، جامعة الموصل، نينوى، العراق

معلومات الارشفة

تاريخ الارشفة:

تاريخ الاستلام :أبريل 4، 2025

تاريخ المراجعة :يونيو 5، 2025

تاريخ القبول :يونيو 24، 2025

تاريخ النشر: الإلكتروني :يوليو 1، 2025

الكلمات المفتاحية:

تحاليل السرعة

المسامية

الكثافة

المعادلات التجريبية

الحقل النفطي

المراسلة:

الاسم: **معن حسن عبد الله**

maan.abdalla@uomosul.edu.iq

الملخص

الدراسة الحالية تتعامل مع معادلات رياضية تجريبية تربط بين الكثافة والمسامية مع العمق. بعد الحصول على معلومات الكثافة والمسامية من تسجيلات خمسة آبار في حقل شرق بغداد النفطي تم إستحداث معادلات تجريبية (مسامية – عمق , كثافة – عمق) للتكاوين الجيولوجية ضمن الفترة بين تكويني (الفتحة – الحارثة) وذلك لغرض مقارنتها مع المعلومات المأخوذة من تحاليل السرع الزلزالية بين عاكسي الفتحة والحارثة. معامل الإرتباط (R) لتلك المعادلات المستنتجة للتكاوين المختلفة يتراوح بين (0.06 – 0.87) والذي أعزي إلى التغيرات الليثولوجية ضمن التكوين الواحد مع العمق. تم تطبيق هذه المعادلات على معلومات العمق المأخوذة من 126 موقع لتحاليل السرع موزعة على شبكة من الخطوط الزلزالية في حقل شرق بغداد النفطي. تم حساب معدلات الكثافة والمسامية للفترة (فتحة – حارثة) باستخدام معادلات مستنبطة. من ثم تم تطبيقها على مستوى الحقل لغرض الحصول على خرائط كنتورية للمسامية والكثافة لهذه الفترة التي أظهرت أنطقة المسامية العالية وعلاقتها مع التجمعات النفطية في الحقل.

DOI: **********,

Introduction

The East Baghdad oil field is located in the centre of Iraq in Baghdad governorate, 10 km east of Baghdad city (Fig. 1). The area of the field is about 120 Km in length and between 20 to 30 Km in width (Al-Ameri & Al-Obaydi, 2011). East Baghdad oil field extends toward Northwest – Southeast from Taji area, Northwest of Baghdad to North of Al-Saouira city in the Southeast of Baghdad. East Baghdad Field is a group of oil fields, which were discovered in 1976, and the first production for it was in 1980. Many oil wells were drilled in that field, which reached the formations of the Cretaceous, and one of them penetrated all Cretaceous Formations and reached the Chia Gara Formation of Upper Jurassic (Harding & Lowell, 1979).

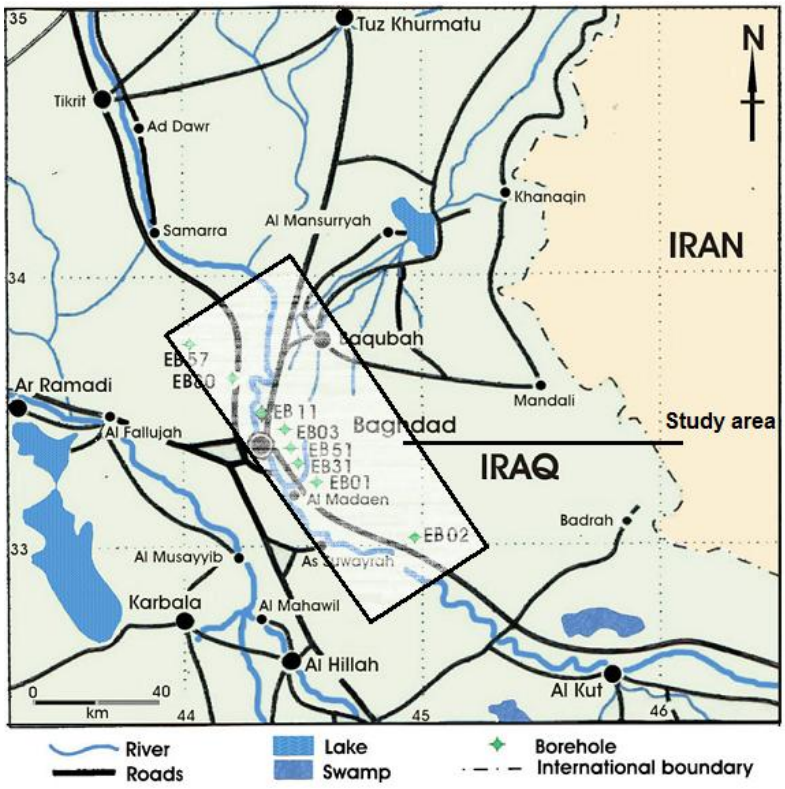

Fig. 1: Location map of the study area (Al-Ameri & Al-Obaydi, 2011).

This region was undergoing tectonic activities with regressive and transgressive cycles that allowed the preservation of high organic matters, leading to the advancement of the biggest oil and gas reserves in the Arabian Region (Sharland et al., 2001). There are many faults in the field with NW-SE trending structure, with oil production which comes from the late Cretaceous Tanuma Formation, fractured carbonates of Khasib Formation and from the early Cretaceous sandstone of Zubair Formation. In other Cretaceous reservoirs, the oil has been successfully checked out, such as the carbonates of Hartha, Mishrif / Rumaila Formations, clastics of Nahr Umr and mixed clastics/carbonate of Ratawi Formations (Al-Ameri & Al-Obaydi, 2011). In the

seismic section, two main faults are appeared (Fig. 2), the first one is normal with NE dipping and it is drilling tops of Ahmadi, Shuaiba, Chia Gara and Gotnia Formations, while the second fault is normal, semi-vertical and it is cutting the tops of same formations that mentioned above. These faults are making a good path allow oil migration along the permeable calcareous sand and shale beds within the Chia Gara Formation in the horizontal movement to a path through faults in vertical movement, and finally reaching the anticline traps. Termination of these traps is filled from the crest to the spill plane, where oil spills below the trap into nearby permeable beds. The spilt oil migrates along tensional joints until it is trapped in the Fatha Anhydrite seal (Al-Ameri & Al-Obaydi, 2011).

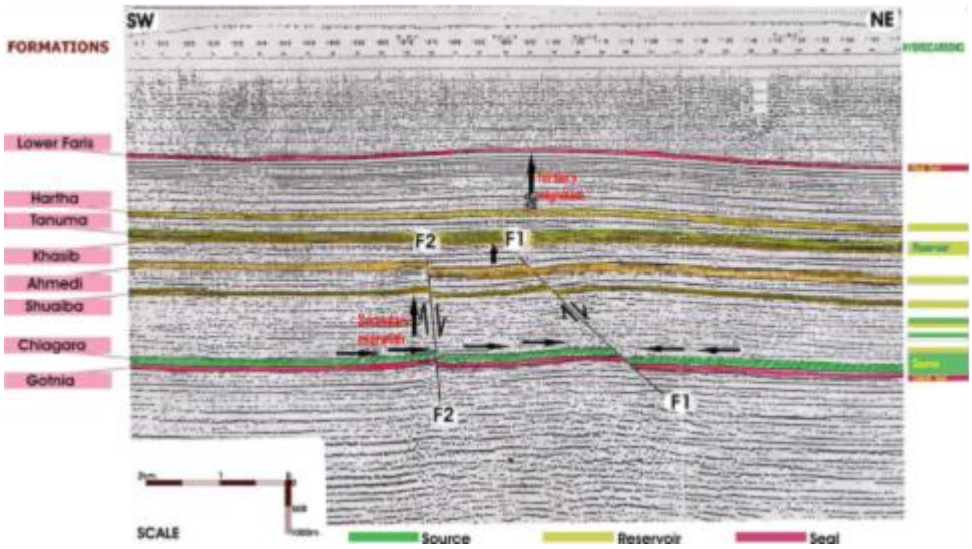

Fig. 2: Seismic cross section played with hydrocarbon source, reservoir, and seal rock units in East Baghdad Oil Field. Double lines indicate directions of migration pathways, while F1 and F2 are normal faults (Al-Ameri & Al-Obaydi, 2011).

Darweesh, Obed and Albadran investigated the structural history of the East Baghdad oil field and indicated that the structural complexity results from oblique-slip growth faults and later folding and faulting (Darweesh et al., 2017). The stratigraphic section consists of many types of rocks which were deposited in marine and lagoon environments, such as carbonates, shale, anhydrite, marl, sandstone, and siltstone. These deposits are expanding in geologic time from Jurassic, Cretaceous, up to Pliocene (Al-Ameri & Al-Obaydi, 2011). (Fig. 3) shows the stratigraphic section of the formations in this field with depth (in m).

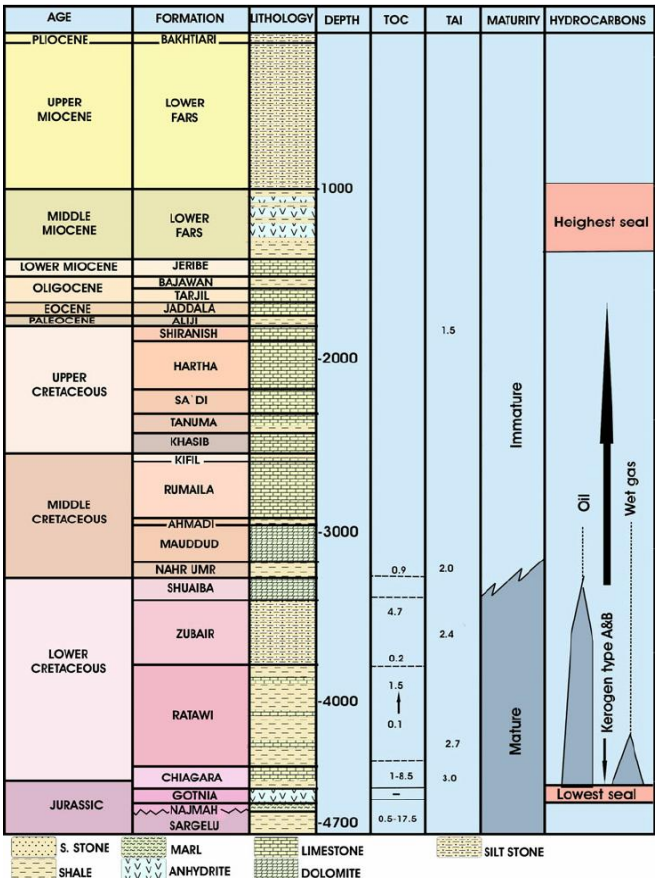

Fig. 3: The stratigraphic section for the East-Baghdad oil field in the study area (Al-Ameri & Al-Obaydi, 2011).

Petrophysical Properties

Velocity-porosity relationships are critical to the determination of lithology from seismic or sonic log data, as well as for direct seismic information of pore fluids. The most important parameters influencing primary porosity are compaction and leaching (Wolf & Chilin, 1976; Kharaka & Berry, 1976; Schmidt et al., 1977). The porosity of a zone can be estimated either from a single porosity log or a combination of porosity logs to correct for variable lithology effects in complex reservoirs (Ebrahim et al., 2023). In the carbonates, mineral mixtures are primarily drawn from calcite, dolomite, and quartz (either as sand grains or as chert); anhydrite and gypsum may also occur. The decrease of porosity with depth can be thought of as a variation of porosity with pressure. Pore pressure can help to preserve porosity at great depths above the top of the overpressure zone. Within a specific depth and lithology, porosity is influenced by confining pressure as pointed out by (Telford et al, 1976). Fuchtbauer has pointed out that the presence of hydrocarbons also preserves porosity (Fuchtbatter, 1967). The rocks of the current study zone contain water, gas and oil, the percentage of which is closely related to the porosity and thickness of the reservoir. The equation was established by Dieokuma. Gu Han and Uko for the porosity trend of two Wells (Dieokuma et al., 2014) is:

$Z = -138.76\ \phi_z + 12383$ --------- (1).

Where: z = depth, and ϕ_z = porosity at given depth.

This implies that, in the absence of a core sample or any porosity, ϕ_Z, can be estimated at any depth, Z, in feet in the area of study.

The purpose of this study is divided into three major aims.

1. Creation of an empirical equation (Density-depth, Porosity-depth) to calculate the porosity and density for all formations within (Fatha- Hartha) interval using well log information.
2. Calculation of the porosity and density values for that period in the whole field using the new empirical equations derived from this study.
3. Later, the maps of both porosity and density for the period (Fatha-Hartha) interval will be established.

MATERIALS AND METHODS

The collected data used in this work have been obtained from two main sources. The first is based on the analysis of seismic data taken from (Dieokuma et al., 2014). These data include (126) velocity analyses scattered at a net of 22 seismic lines. The second is obtained from the log data for five wells scattered in the north part of the east Baghdad oil field.

Data Sources

1-Velocity analyses Data

The seismic data of two reflectors (Fatha, Hartha) are obtained from the RMS velocity analyses to 126 locations scattered in the East Baghdad oil field (Fig. 4) (Dieokuma et al., 2014). These data contain the depths (Z) of both reflectors, which were derived from seismic velocity information.

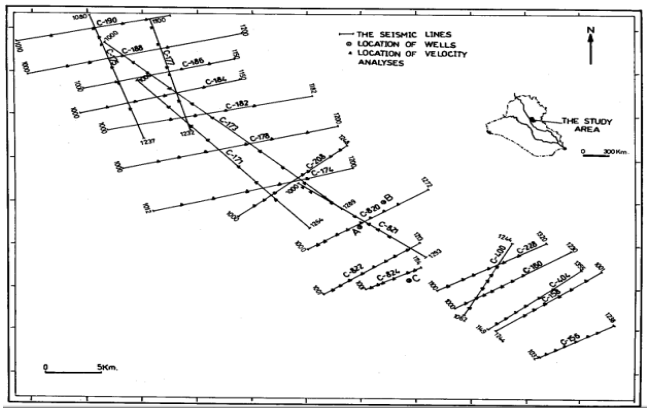

Fig. 4: Location map of the seismic lines in the study area (Dieokuma et al., 2014).

2- Well Logs Data

The well log data for five wells (EB02, EB04, EB16, EB34, and EB88) were obtained from the Iraqi Ministry of Oil. These data include different information about the petrophysical properties of the reservoir. In order to determine porosity values with greater accuracy, corrections must be made for the shaliness. The corrections of Neutron-density readings for the shale effect are made after estimating shale volume from the Gamma ray. Corrections of the log readings in this study were made by using the Interactive Petrophysics program (IP) to carry out environmental corrections. (Fig. 5) shows one of the well log records used in this study.

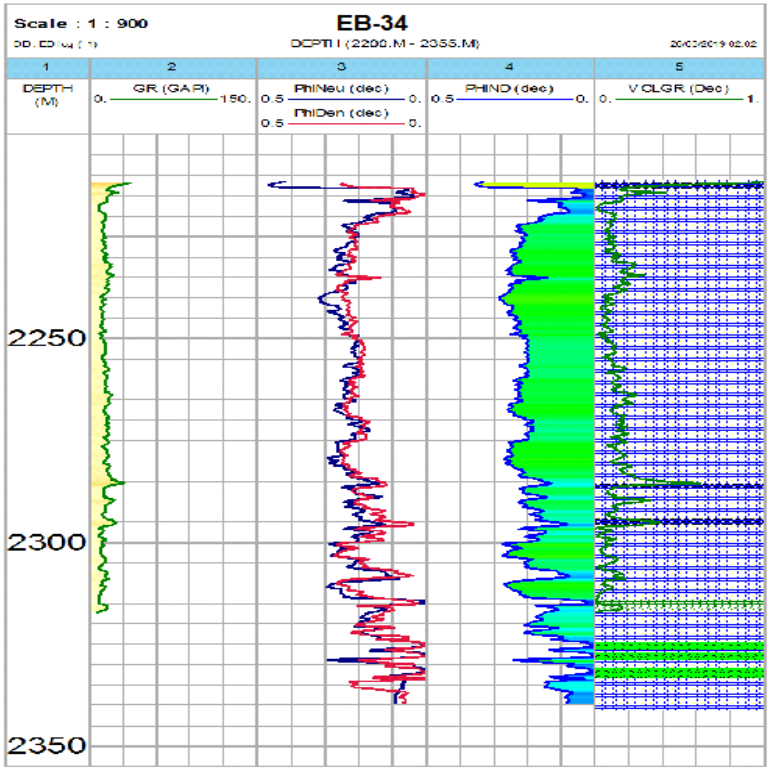

Fig. 5: The corrected well log data for well (EB-34).

By the following relationships, the corrections of Neutron, Density, and Sonic logs were performed to derive porosity:

$\phi N_{corr} = \phi N-(V_{sh}*\phi N_{sh})$ ---------- (4)

$\phi D_{corr} = \phi D-(V_{sh}*\phi D_{sh})$ ---------- (5)

$\phi N.D = (\phi N+\phi D)/2$ ---------- (6).

Where:

V_{sh} = the shale volume, ϕN_{sh} = the neutron porosity in shale formation, and ϕD_{sh} = the density porosity in shale formation.

RESULTS

The New Empirical Equation of the Study Area

The (Porosity-depth, Density-depth) equations for all the formations within (Fatha-Hartha interval were predicted based on porosity, density, and depth data obtained from well logs of the five wells mentioned above. These equations were produced using the Excel program V.10. Later, the optimum empirical equations (Porosity-Depth, Density-Depth) for the (Fatha – Hartha) period were deduced and generalized to all parts of the field.

Fatha – Hartha Interval

This interval consists of nine formations in its stratigraphic column (well log data), which are Fatha, Jeribe, Dhiban, Bajwan, Tarajil, Palani, Jadala, Aaliji, and Shiranish. The following is a brief description of all formations in this interval and their new empirical equations:

1-Fatha Formation

This formation appeared as cyclic alterations of Anhydrite, Limestone, Marl, Claystone and Salt rocks. It extends between the depths (813m and 1195m) with a thickness (382 m. The porosity and density relationships with the depth of this formation and their parameters are shown in the figures (6,7).

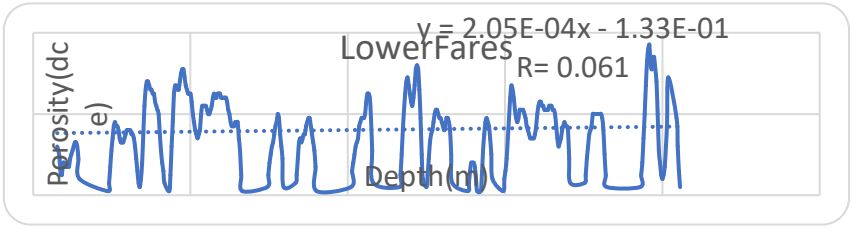

Fig. 6: The porosity-depth relationship of the Fatha Formation and its parameters.

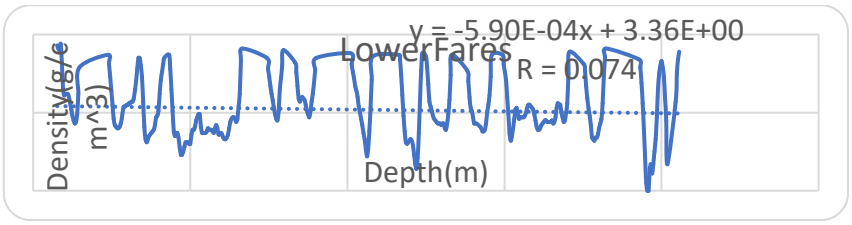

Fig. 7: The density-depth relationship of the Fatha Formation and its parameters.

2- Jeribe Formation

The formation consists of Dolomitic Limestone and Anhydrite, which extends between depths (1195 m –1250 m) with a thickness (55m). The porosity and density relationships with the depth of this formation and their parameters are shown in the figures (8,9).

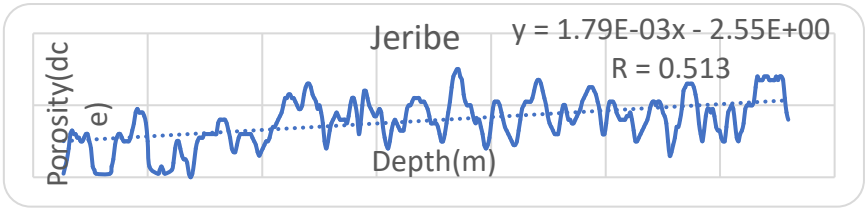

Fig. 8: The porosity-depth relationship of the Jeribe Formation and its parameters.

Fig. 9: The density-depth relationship of the Jeribe Formation and its parameters.

3 - Dhiban Formation

This formation consists of Dolomitic Limestone and Anhydrite, which extends between depths (1250m – 1333.5m) with a thickness (83.5m. The porosity and density relationships with the depth of this formation and their parameters are shown in the figures (10,11).

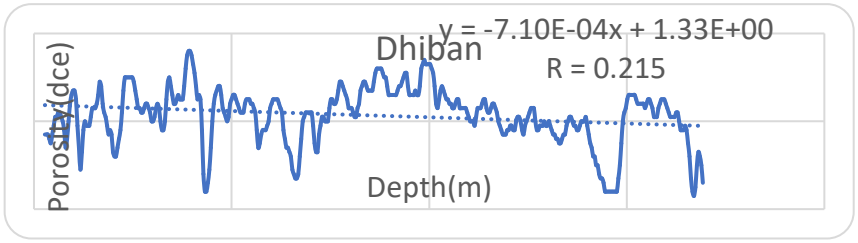

Fig. 10: The porosity-depth relationship of the Dhihban Formation and its parameters.

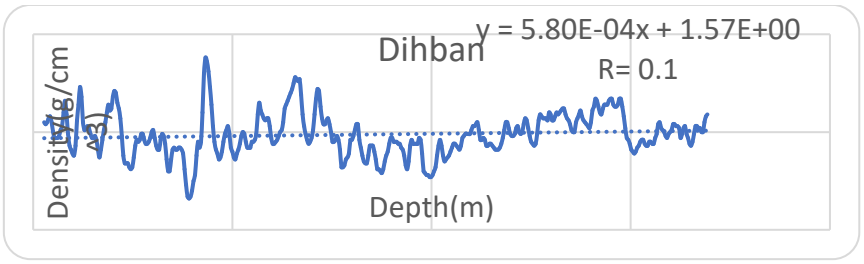

Fig. 11: The density-depth relationship of Dhihban Formation and its parameters.

4- Bajwan/Baba Formation

Dolomite and Limestone were only included in this formation that extended between depths (1333.5 m – 1360.5m) with a thickness (27m. The porosity and density relationships with the depth of this formation and their parameters are shown in the figures (12,13).

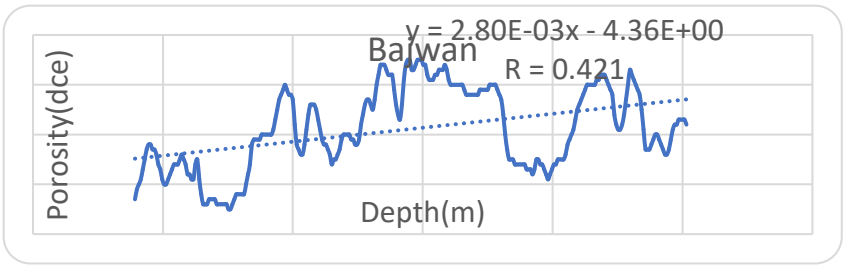

Fig. 12: The porosity-depth relationship of the Bajwan/Baba Formation and its parameters.

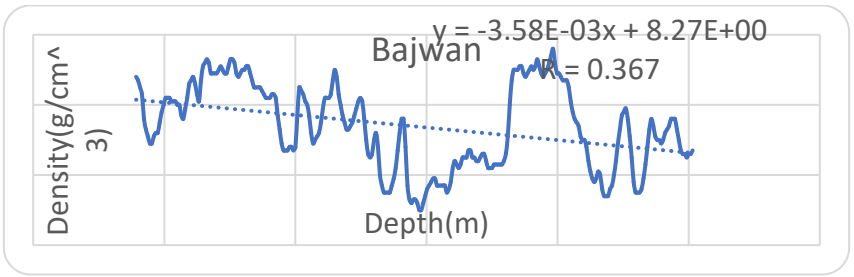

Fig. 13: The density-depth relationship of the Bajwan/Baba Formation and its parameters.

5- Tarjil Formation

The main rock type in this formation is Limestone which extends between depths (1360.5 m – 1401.5 m) with a thickness (41m. The porosity and density relationships with the depth of this formation and its parameters are shown in the figures (14,15).

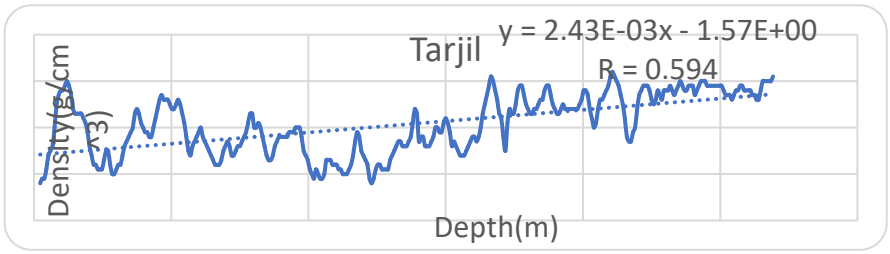

Fig. 14: The porosity-depth relationship of the Tarjil Formation and its parameters.

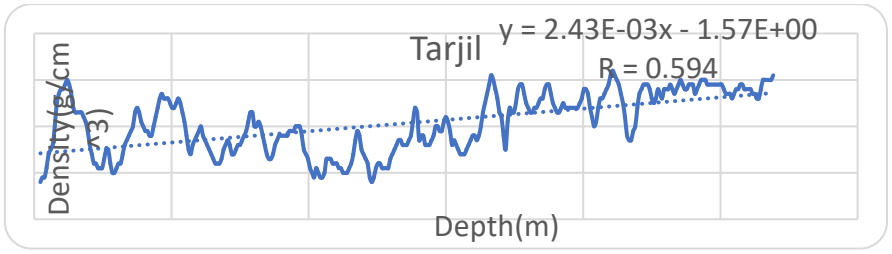

Fig. 15: The density-depth relationship of the Tarjil Formation and its parameters.

6- Palani Formation

Limestone is the main rock type in this formation that is restricted between depths (1401.5 m – 1486 m, with a thickness (84.5m. The porosity and density relationships with the depth of this formation and their parameters are shown in the figures (16,17).

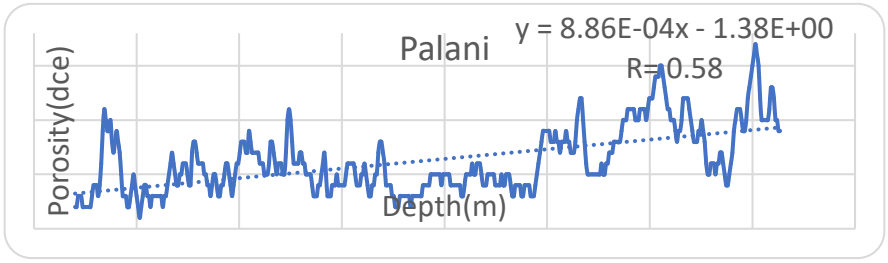

Fig. 16: The porosity-depth relationship of Palani Formation and its parameters.

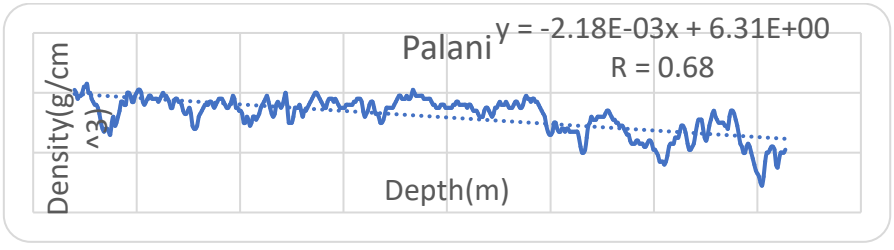

Fig. 17: The density-depth relationship of Palani Formation and its parameters.

7- Jaddala Formation

Limestone was only contained in this formation and extends between depths (1486 m – 1547 m) with a thickness (61m. The porosity and density relationships with the depth of this formation and its parameters are shown in the figures. (18,19).

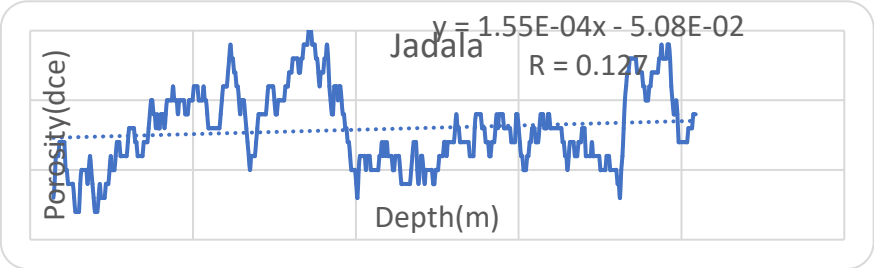

Fig. 18: The porosity-depth relationship of the Jaddala Formation and its parameters.

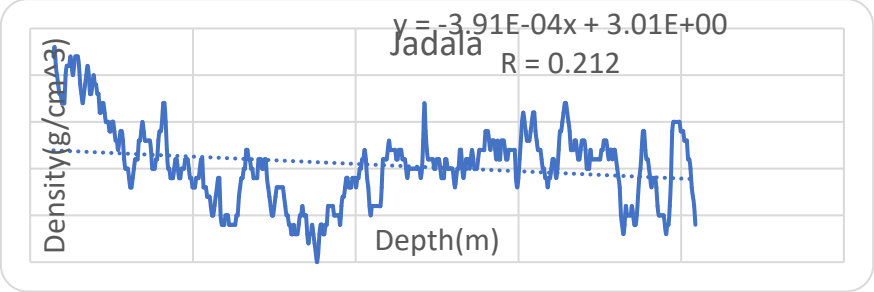

Fig. 19: The density-depth relationship of the Jaddala Formation and its parameters.

8- Aaliji Formation

Limestone represents the main rock type in Aaliji Formation, which extends between depths (1547 m – 1577 m) with a thickness (30m. The porosity and density relationships with the depth of this formation and their parameters are shown in the figures (20,21).

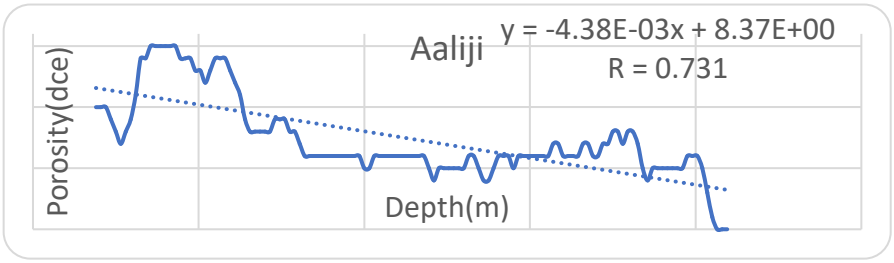

Fig. 20: The porosity-depth relationship of the Aaliji Formation and its parameters.

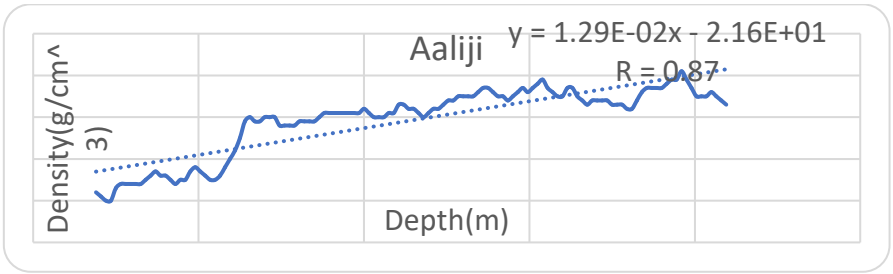

Fig. 21: The density-depth relationship of Aaliji Formation and its parameters.

9- ShIranian Formation

Limestone, Arg. Limestone and Shale are only included in this formation, which extends between depths (1577 m – 1632 m) with a thickness (55 m. There is not enough data about this formation in the well logs except for a few meters (5m - 6m). Later, the porosity and density relationships with the depth of the whole interval (Fatha-Hartha) were established as shown in figures (22,23).

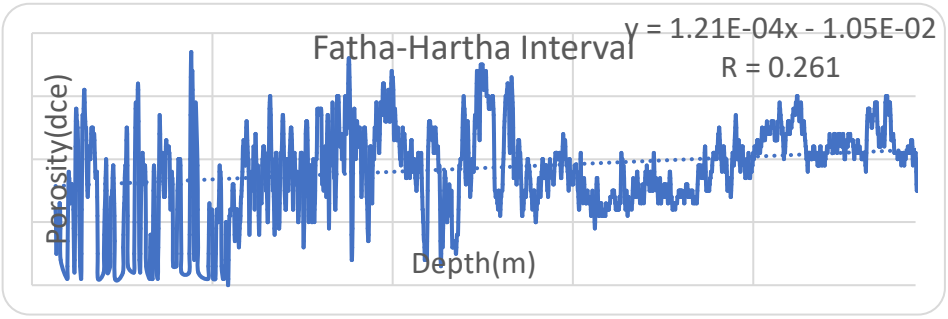

Fig. 22: The porosity-depth relationship of the (Fatha-Hartha) interval and its parameters.

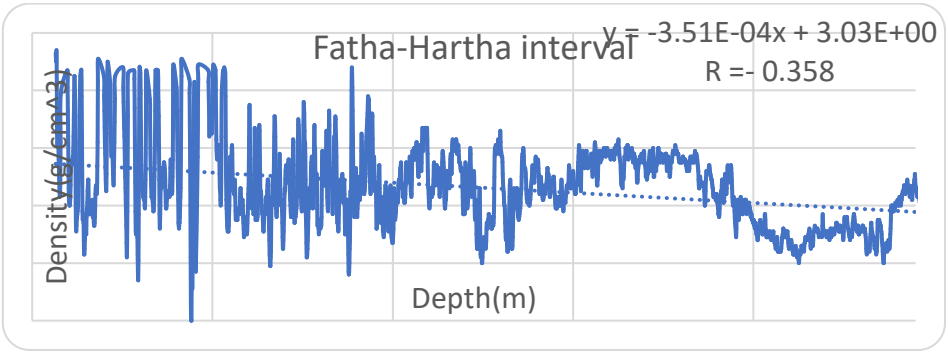

Fig. 23: The Density-depth relationship of (Fatha-Hartha) interval and its parameters.

$y = 1.21* 10^{-4} x - 1.05*10^{-2}$----------(7) Equation of porosity

Where Y is the porosity in (%), and X is the depth in (m).

$y = -3.51*10^{-4} x + 3.03$ ----------(8) Equation of density

Where Y is the density in (g/cm^3), and X is the depth in (m).

These two equations are applied on the depths of two reflectors (Fatha, Hartha) in the whole field (Table1) to produce the average porosity and density maps for this interval (Table 2) figures (24, 25).

Table 1: The depths values of Fatha and Hartha reflectors for all shot points (SP.) in the study area

Line no.	Sp.	Depth m		Line no.	Sp.	Depth m		Line no.	Sp.	Depth m	
		F.	H.			F..	H.			F.	H.
	1266	700	1050		1132	635	980		1189	750	1070
	1242	678	1055		1107	630	970		1158	730	1060
173A	1216	675	1050	173B	1082	630	950		1137	715	1050
	1192	670	1040		1055	615	955	822	1112	715	1055
	1026	590	955		1032	610	955		1090	715	1050
	1046	590	955		1042	550	930		1061	710	1055
	1070	590	950		1080	565	1000		1037	705	1050
	1110	585	970	190	1104	605	1000		1018	700	1035
175	1118	590	970		1128	625	1015		1080	750	1070
	1148	595	980		1160	655	1040		1105	750	1080
	1166	585	975		1126	665	1055	400	1130	780	1080
	1200	600	970	186	1102	645	1030		1150	820	1130
	1132	642	1030		1074	620	1010		1163	840	1160
188	1088	610	995		1036	575	970		1184	830	1180
	1058	570	950		1156	680	1030		1168	750	1100
	1034	575	915		1130	675	1015		1188	765	1090
	1028	695	1005	174	1100	650	995	404	1209	790	1110
	1048	690	1015		1068	620	965		1228	830	1140
	1072	700	1020		1038	580	905		1258	870	1200
820	1097	730	1025		1184	660	1030		1288	900	1255
	1123	700	1030		1162	645	1010		1134	685	1060
	1148	715	1050		1136	640	1020	182	1108	650	1035
	1176	740	1070	171	1098	625	1010		1080	620	1020
	1205	775	1100		1074	610	1000		1056	615	1000
	105	740	1100		1044	615	1005		1026	570	940
	1075	775	1110		1098	700	1065	184	1052	600	980
	1100	820	1150		1081	700	1055		1080	630	1010
156	1130	855	1200		1058	700	1050		1116	650	1030
	1160	900	1250	824	1035	700	1040		1085	625	955
	1185	920	1270		1024	710	1040	177	1110	635	980
158	1030	880	1280		1011	710	1030		1130	640	990

	1070	875	1250		1210	700	1050		1160	635	990
	1100	855	1240		1185	700	1050		1187	635	990
	1135	810	1190		1163	690	1050		1200	620	980
	1160	775	1170	821	1126	700	1040		1120	720	1080
	1180	765	1150		1079	690	1040		1150	725	1080
	1022	750	1080		1036	690	1050	228	1170	735	1090
	1054	760	1085		1015	690	1055		1200	785	1130
168	1070	775	1105		1031	580	1005		1230	820	1190
	1090	800	1150		1025	610	1015		1260	850	1225
	1110	840	1180	178	1077	630	1035				
	1130	865	1210		1115	655	1065				
					1139	670	1100				
					1170	740	1150				

Table 2: The average values of Porosity and density for all shot points (SP.) in the study area

Line No.	SP. No.	Φ in dec.	ρ in gm/cc	line No.	SP. No.	Φ in dec.	ρ in gm/cc	Line No.	SP. No.	Φ in dec.	ρ in gm/cc
	1266	0.176	2.49		1038	0.172	2.501		1134	0.172	2.499
	1242	0.184	2.467		1120	0.171	2.502	182	1108	0.175	2.493
173A	1216	0.182	2.47		1150	0.165	2.522		1080	0.166	2.517
	1192	0.176	2.49	228	1170	0.17	2.507		1056	0.171	2.503
	1026	0.158	2.542		1200	0.183	2.469		1026	0.153	2.555
	1046	0.155	2.551		1230	0.199	2.424	184	1052	0.17	2.507
	1070	0.154	2.552		1260	0.207	2.399		1080	0.169	2.509
175	1110	0.157	2.545		1080	0.177	2.486		1116	0.175	2.492
	1118	0.16	2.535		1105	0.168	2.513		1085	0.154	2.552
	1148	0.162	2.531	400	1130	0.172	2.5		1110	0.165	2.52
	1166	0.162	2.529		1150	0.183	2.468	177	1130	0.156	2.546
	1200	0.162	2.53		1163	0.204	2.408		1160	0.159	2.54
	1132	0.176	2.489		1184	0.192	2.441		1187	0.163	2.526
188	1088	0.168	2.513		1168	0.19	2.449		1200	0.159	2.538
	1058	0.158	2.541		1188	0.181	2.474		1189	0.173	2.498
	1034	0.149	2.568	404	1209	0.185	2.462		1158	0.174	2.495
	1028	0.16	2.535		1228	0.201	2.417		1137	0.162	2.531
	1048	0.166	2.517		1258	0.211	2.389	822	1112	0.17	2.505
	1072	0.165	2.522		1288	0.224	2.349		1090	0.168	2.513
820	1097	0.159	2.537		1132	0.156	2.546		1061	0.167	2.514
	1123	0.155	2.55	173B	1107	0.155	2.55		1037	0.175	2.491
	1148	0.168	2.513		1082	0.151	2.561		1018	0.168	2.512
	1176	0.17	2.506		1055	0.151	2.563		1134	0.172	2.499
	1205	0.174	2.495		1032	0.149	2.566	182	1108	0.175	2.493
	105	0.187	2.457		1042	0.144	2.581		1080	0.166	2.517
	1075	0.188	2.454	190	1080	0.159	2.537		1056	0.171	2.503
156	1100	0.196	2.431		1104	0.155	2.55		1026	0.153	2.555
	1130	0.209	2.393		1128	0.167	2.516	184	1052	0.17	2.507
	1160	0.225	2.348		1160	0.167	2.514		1080	0.169	2.509
	1185	0.223	2.351		1126	0.169	2.508		1116	0.175	2.492
	1030	0.226	2.345	106	1102	0.168	2.514		1085	0.154	2.552
	1070	0.214	2.378		1074	0.161	2.532		1110	0.165	2.52
158	1100	0.22	2.362		1036	0.159	2.538	177	1130	0.156	2.546
	1135	0.212	2.386		1156	0.18	2.478		1160	0.159	2.54
	1160	0.201	2.415		1130	0.172	2.5		1187	0.163	2.526
	1180	0.202	2.413	174	1100	0.171	2.504		1200	0.159	2.538
	1022	0.182	2.472		1068	0.175	2.493		1189	0.173	2.498
160	1054	0.188	2.455		1038	0.16	2.536	822	1158	0.174	2.495
	1070	0.19	2.449	171	1184	0.17	2.505		1137	0.162	2.531

	1090	0.189	2.451		1162	0.166	2.517		1112	0.17	2.505
	1110	0.212	2.385		1136	0.172	2.5		1090	0.168	2.513
	1130	0.205	2.405		1098	0.175	2.492		1061	0.167	2.514
	1235	0.192	2.442		1074	0.165	2.521		1037	0.175	2.491
	1212	0.189	2.45		1044	0.17	2.507		1018	0.168	2.512
	1160	0.185	2.464		1098	0.163	2.526				
206	1148	0.178	2.483		1081	0.174	2.495				
	1084	0.179	2.48	824	1058	0.163	2.528				
	1060	0.172	2.502		1035	0.171	2.505				
	1185	0.125	2.638		1024	0.171	2.505				
	1163	0.174	2.494		1025	0.171	2.502				
821	1126	0.173	2.497		1031	0.175	2.492				
	1079	0.173	2.498	178	1077	0.177	2.487				
	1036	0.18	2.477		1115	0.179	2.481				
	1015	0.174	2.495		1139	0.183	2.47				
					1170	0.189	2.451				

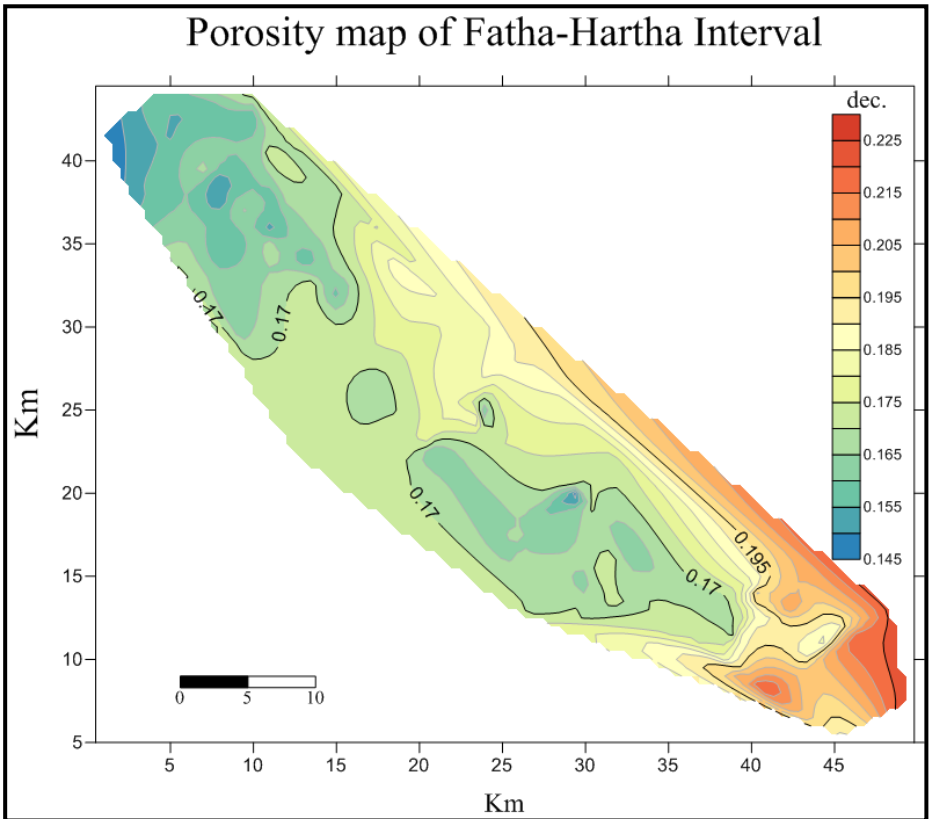

Fig. 24: porosity map of the Fatha-Hartha interval in the study Area.

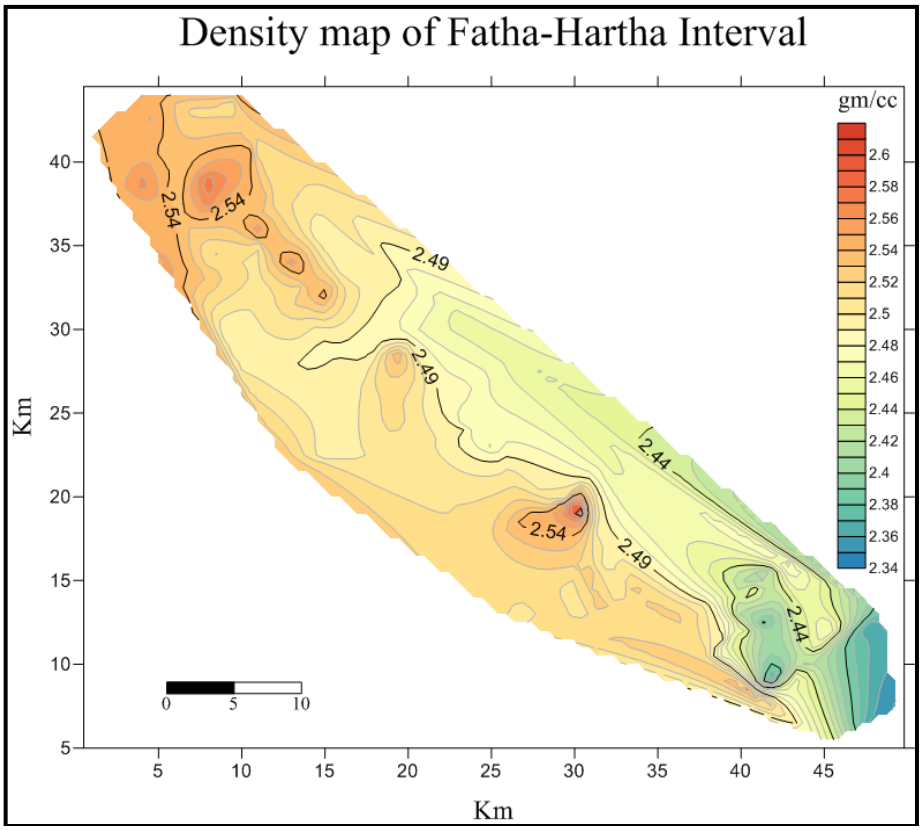

Fig. 25: Density map of Fatha - Hartha interval in the study area.

DISCUSSION

The log interpretations have been carried out using the Interactive Petrophysics Program (IP) and show that the formations consist mainly of limestone with the inclusion of dolomite, anhydrite, siltstone, shale, marl, claystone, and salt rocks. In the present study, the porosity and density equations with depth were determined using the well logs data. After applying these equations to the seismic velocity analyses information for 126 sites, the average porosity and density contour maps for the (Fatha- Hartha) period have been produced. The correlation coefficient (R) of these equations ranges from weak (0.011) to strong (0.87), depending on the consistency of porosity and density within the formation. The low R values in formations (Fatha, Dhiban, and Jaddala) can be due to the heterogeneity of formation components, while their high values in Aaliji and Shiranish Formations may be caused by homogeneity. Although the value of R in the equation of period (Fatha - Hartha) is relatively small, it can be valid for calculating porosity and density rates with depth for whole area. In this interval, the porosity distributes gradually. It reaches 11.5% in the southern part, while it increases to (18%-22%) in the middle parts and increases gradually towards the northeast to be (25%). The density has a reverse behaviour as it increases in the southern part and decreases northwards. In spite of the thickness of the sediment increasing in the south-east part of the study area (According to (Al-Ameri & Al-Obaydi, 2011)), porosity is increasing in this direction.

CONCLUSION

1. This study deduces new equations (porosity-depth, density-depth) for all formations in (Fatha - Hartha). seismic interval using well log data.
2. Establishing the average porosity and density maps for that period in the study area by applying the new equations on 126 velocity analysis sites.
3. The value of R can be used as a function of homogeneity among formation components.
4. Increased porosity values toward the south-eastern part of the study area despite increased sediment thickness, which may give information on the change of lithological facies or possibly increase hydrocarbon concentrations in that direction.

ACKNOWLEDGMENT

The author is grateful to the University of Mosul College of Petroleum and Mining Engineering for providing access to their facilities, which greatly helped to improve the quality of this research.

References:

Al-Ameri, T. K., & Al-Obaydi. (2011). Khasib and Tannuma oil sources, East Baghdad oil field, Iraq. Marine and Petroleum Geology, 28, 880–894.

Al-Majid, M. H. (1992). The study of compaction in the East Baghdad oil field by using seismic velocity analyses [Unpublished master's thesis]. University of Mosul, Iraq.

Darweesh, H. A., Obed, A. M., & Albadran, B. N. (2017). Structural study of East Baghdad oil field. World Journal of Engineering Research and Technology, 3(6), 56–66.

Dieokuma, T., Gu, H. M., & Uko, E. D. (2014). Porosity modeling of the South-East Niger Delta Basin, Niger. International Journal of Geology, Earth and Environmental Sciences, 4.

Ebrahim, D. M., Al-Majid, M. H., Al-Hamidi, R. E., & Al-Hamdani, S. A. (2023). Porosity type determination using the velocity deviation technique for the Sheikh Allas Formation in the Kirkuk Oil Field, Northeastern Iraq. Iraqi National Journal of Earth Science, 23(2), 20–36.

Fuchtbauer, H. (1967). Influence of different types of diagenesis on sandstone porosity. In Proceedings of the 7th World Petroleum Congress (Vol. 2, pp. 353–369).

Harding, T. P., & Lowell, J. D. (1979). Structural styles, their plate-tectonic habitats, and hydrocarbon traps in petroleum province. AAPG Bulletin, 63, 1016–1058.

Kharaka, Y. K., & Berry, E. A. E. (1976). Chemistry of waters expelled from sands and sandstones. In G. V. Chilingarian & K. H. Wolf (Eds.), Compaction of Coarse-Grained Sediments II (pp. 41–68). Elsevier.

Schmidt, V., McDonald, D. A., & Platt, R. L. (1977). Pore geometry and reservoir aspects of secondary porosity in sandstones. Bulletin of Canadian Petroleum Geology, 25, 271–290.

Sharland, P. R., Archer, R., Casey, D. M., Davies, R. B., Hall, S. H., Heward, A. P., Horbery, A. D., & Simmons, M. D. (2001). Arabian Plate sequence stratigraphy. Gulf PetroLink.

Telford, W. M., Geldart, L. P., & Sheriff, R. E. (1976). Applied geophysics (2nd ed.). Cambridge University Press.

Wolf, K. H., & Chilin, A. G. (1976). Diagenesis of sandstones and compaction. In G. V. Chilingarian & K. H. Wolf (Eds.), Compaction of Coarse-Grained Sediments II (pp. 69–444). Elsevier.